

Decentralized Rendezvous of Nonholonomic Robots with Sensing and Connectivity Constraints

Zhen Kan ^a, Justin Klotz ^a, Eduardo L. Pasiliao Jr ^b, John M. Shea ^c,
Warren E. Dixon ^a,

^a*Department of Mechanical and Aerospace Engineering, University of Florida, Gainesville, USA*

^b*Munitions Directorate, Air Force Research Laboratory, Eglin AFB, FL 32542, USA.*

^c*Department of Electrical and Computer Engineering, University of Florida, Gainesville, USA*

Abstract

A group of wheeled robots with nonholonomic constraints is considered to rendezvous at a common specified setpoint with a desired orientation while maintaining network connectivity and ensuring collision avoidance within the robots. Given communication and sensing constraints for each robot, only a subset of the robots are aware or informed of the global destination, and the remaining robots must move within the network connectivity constraint so that the informed robots can guide the group to the goal. The mobile robots are also required to avoid collisions with each other outside a neighborhood of the common rendezvous point. To achieve the rendezvous control objective, decentralized time-varying controllers are developed based on a navigation function framework to steer the robots to perform rendezvous while preserving network connectivity and ensuring collision avoidance. Only local sensing feedback, which includes position feedback from immediate neighbors and absolute orientation measurement, is used to navigate the robots and enables radio silence during navigation. Simulation results demonstrate the performance of the developed approach.

1 Introduction

Distributed cooperative control of networked multi-agent systems has attracted considerable interest. One particular cooperative control problem is the rendezvous problem, where a number of agents arrive at a predefined destination simultaneously, ideally using limited information from the environment and team members. Some example applications of the rendezvous problem are cooperative strike and cooperative jamming in [1] and [2]. In the cooperative strike scenario, multiple strikes are executed on a target simultaneously by firing from different locations. In cooperative jamming of a wireless communication network with eavesdroppers, noisy signals are transmitted to jam the eavesdroppers at the

same time when the source transmits the message signal. Spacecraft docking, air-to-air refueling, and the interception of an incoming missile can also be considered as rendezvous problems. In these applications, coordination and collaboration are crucial to performance, and agents are required to communicate and coordinate their movements with others to achieve rendezvous.

Several rendezvous results are reported in [3–5]. Convergence to a common point for a group of autonomous mobile agents is studied in [3]. In [4] and [5], synchronized and unsynchronized strategies are developed to drive mobile agents to a single unspecified location by using only position feedback from its sensing regions. A common assumption in [3–5] is that the network remains connected during the motion evolution, allowing constant interaction between agents. However, the assumption of network connectivity is not always practical. Typically, each agent can only make decisions based on the local information from immediate neighbors within a certain region due to sensing and communication constraints. Since communication/sensing links generally depend on the distance between agents, agent motion may cause the underlying network to disconnect. If the network disconnects, certain agents may no longer be able to commu-

Email addresses: kanzhen0322@uf1.edu (Zhen Kan), jklotz@uf1.edu (Justin Klotz), pasiliao@eglin.af.mil (Eduardo L. Pasiliao Jr), jshea@ece.ufl.edu (John M. Shea), wdixon@uf1.edu (Warren E. Dixon).

¹ This research is supported in part by NSF award numbers 1161260, 1217908, and a contract with the AFRL Mathematical Modeling and Optimization Institute. Any opinions, findings and conclusions or recommendations expressed in this material are those of the authors and do not necessarily reflect the views of the sponsoring agency.

nicate and coordinate their motion, leading to a failure of cooperative tasks.

Recent results such as [6–11] have focused on maintaining network connectivity when performing rendezvous tasks. A circumcenter algorithm is proposed in [6] to avoid the loss of existing links between agents. In [7–9] a potential field-based distributed approach is developed to prevent partitioning in the underlying graph by using local information from each agent’s immediate neighbors. The results in [10] provide a connectivity-preserving protocol for rendezvous of a discrete-time multi-agent system, and a hybrid dynamic rendezvous protocol is designed in [11] to address finite-time rendezvous problems while preserving network connectivity. However, most of the aforementioned works only consider linear motion models. Although agents with nonholonomic kinematics are considered in [7], like other results such as [3–5, 11], the agents can only converge to a destination determined by the initial deployment. A dipolar navigation function was proposed and a discontinuous time-invariant controller was developed for a multi-robot system in [12] to perform nonholonomic navigation for networked robots. The dipolar navigation function is a particular class of potential functions, which is developed from [13] and [14] such that the negative gradient field does not have local minima, and the closed-loop navigation function guarantees convergence to the global minimum. The result in [12] was then extended to navigate a nonholonomic system in three dimensions in [15]. Other recent results focused on nonholonomic systems with various cooperative tasks such as formation control and flocking are reported in [16–19]. However, network connectivity is not considered in [12, 15–19].

The rendezvous problem for mobile robots with nonholonomic constraints is studied in this work, and the objective is to reach a common specified setpoint with a desired orientation. Only a small subset of robots (i.e., informed agents) are assumed to be equipped with advanced sensors (e.g., GPS) and provided with global knowledge of the destination, while the remaining robots (i.e., followers) only have a range sensor (e.g., a passive range sensor such as a camera, or active sensors such as sonar, laser, or radar), which provides local feedback of the relative trajectory of other robots within a limited sensing region. Since the follower robots are not aware of the global position of the destination, they have to stay connected with the informed agents when performing rendezvous. To avoid collision among robots, the workspace is divided into a collision-free region and a rendezvous region. Particularly, the robots are required to avoid collisions with other robots outside a neighborhood of the common goal. Based on our preliminary efforts in [20–22], a decentralized time-varying controller, using only local sensing feedback from its immediate neighbors, is designed to stabilize the robots at the specified destination while preserving network connectivity and ensuring collision avoidance. The devel-

oped decentralized controller only uses local sensing information and no inter-agent communication is required (i.e., communication-free global decentralized group behavior). Although network connectivity is maintained so that radio communication is available when required for various tasks, communication is not required for navigation. Using the navigation function framework, the multi-robot system is guaranteed to rendezvous at a common destination with a desired orientation without being trapped by local minima from almost all initial conditions, excluding a set of measure zero. Compared to [22] where the formation control for a group of agents with fully actuated dynamics is investigated, networked mobile robots with nonholonomic constraints are considered in this work. Unlike our centralized result in [20] or our preliminary result in [21] in which all the robots are required to know the goal destination and only undirected interaction between robots are considered, the current result models the interaction among robots as a digraph, and only requires a subset of the robots (i.e., one or more) to have knowledge of the global position of the destination and the desired orientation. This advancement reduces required resources and sensor loads on the remaining robots. Within this setting, the informed subset of robots can perform a task-level controller, while the remaining robots just execute a local interaction-based strategy. Moreover, the developed controller allows the robots to rendezvous at any desired destination, versus an unspecified destination determined by their initial deployment as in [3–5, 7, 11]. The result can also be extended by replacing the objective function in the navigation function to accommodate different tasks, such as formation control, flocking, and other applications.

2 Problem Formulation

Consider N networked mobile robots operating in a workspace \mathcal{F} , where \mathcal{F} is a bounded disk area with radius R_w . Each robot in \mathcal{F} moves according to the following nonholonomic kinematics:

$$\dot{q}_i = \begin{bmatrix} \cos \theta_i & 0 \\ \sin \theta_i & 0 \\ 0 & 1 \end{bmatrix} \begin{bmatrix} v_i(t) \\ \omega_i(t) \end{bmatrix}, \quad i = 1, \dots, N \quad (1)$$

where $q_i(t) \triangleq [p_i^T(t) \theta_i(t)]^T \in \mathbb{R}^3$ denotes the states of robot i , with $p_i(t) \triangleq [x_i(t) y_i(t)]^T \in \mathbb{R}^2$ denoting the position of robot i , and $\theta_i(t) \in (-\pi, \pi)$ denoting the robot orientation with respect to the global coordinate frame in \mathcal{F} . In (1), $v_i(t)$, $\omega_i(t) \in \mathbb{R}$ are the control inputs that represent the linear and angular velocity of robot i , respectively.

The subsequent development is based on the assumption that all robots have equal actuation capabilities and each

robot has sensing and communication limitations encoded by a disk area with radius R , which indicates that two moving robots can sense and communicate with each other as long as they stay within a distance of R . We also assume that only a subset of the robots, called informed robots, are provided with knowledge of the destination, while the other robots can only use local state feedback (i.e., position feedback from immediate neighbors and absolute orientation measurement). Furthermore, while multiple informed robots may be used for rendezvous, the analysis and results of this work are focused on a single informed robot. The techniques proposed in this work could be extended to the case of multiple informed robots by using containment control, as explained in Remark 2. The interaction among the robots is modeled as a directed graph $\mathcal{G}(t) = (\mathcal{V}, \mathcal{E}(t))$, where the node set $\mathcal{V} = \{1, \dots, N\}$ represents the group of robots, and the edge set $\mathcal{E}(t)$ denotes time-varying edges. The set of informed robots and followers are denoted as \mathcal{V}_L and \mathcal{V}_F , respectively, such that $\mathcal{V}_L \cup \mathcal{V}_F = \mathcal{V}$ and $\mathcal{V}_L \cap \mathcal{V}_F = \emptyset$. Let $\mathcal{V}_L = \{1\}$ and $\mathcal{V}_F = \{2, \dots, N\}$. A directed edge $(i, j) \in \mathcal{E}$ in $\mathcal{G}(t)$ exists between node i and j if their relative distance $d_{ij} \triangleq \|p_i - p_j\| \in \mathbb{R}^+$ is less than R . The directed edge (i, j) indicates that node i is able to access the states (i.e., position and orientation) of node j through local sensing, but not vice versa. Accordingly, node j is a neighbor of node i (also called the parent of node i), and the neighbor set of node i is denoted as $\mathcal{N}_i = \{j \mid (i, j) \in \mathcal{E}\}$, which includes the nodes that can be sensed. A directed spanning tree is a directed graph, where every node has one parent except for one node, called the root, and the root node has directed paths to every other node in the graph. Since the follower robots are not aware of the destination, they have to stay connected with the informed robot either directly or indirectly through concatenated paths, such that the knowledge of the destination can be delivered to all the nodes through the connected network. Hence, to complete the desired tasks, maintaining connectivity of the underlying graph is necessary.

Collision avoidance among robots has not been considered for rendezvous problems in existing literature (e.g., [4–9]), since it conflicts with the objective of meeting at a common goal. To enable collision avoidance in this work, the workspace \mathcal{F} is divided into a collision-free region Ω_c and a rendezvous region Ω_r , such that $\Omega_c \cup \Omega_r = \mathcal{F}$. The rendezvous region Ω_r is a bounded disk area with radius R_r centered at the common destination p^* , while the remaining area in \mathcal{F} is the collision-free region Ω_c . Assume that the workspace \mathcal{F} and the rendezvous region Ω_r satisfy that $R_w \gg R_r$ and $R_r > R(N - 1)$. The classical rendezvous problem enables the robots to rendezvous at p^* with a desired orientation θ^* in Ω_r , we additionally constraint this model by requiring collision avoidance among robots outside the neighborhood of common p^* (i.e., Ω_c). The main contribution of this work is to derive a set of distributed controllers using only local informa-

tion (i.e., position feedback from immediate neighbors and the absolute orientation measurement) to perform rendezvous, ensure network connectivity, and avoid collisions. To achieve these goals, the following assumptions are required in the subsequent development.

Assumption 1 *The initial graph $\mathcal{G}(0)$ has a directed spanning tree with the informed node as the root.*

Assumption 2 *The destination p^* and desired orientation θ^* are achievable, which implies that p^* and θ^* do not coincide with some unstable equilibria (i.e., saddle points).*

3 Control Design

3.1 Dipolar Navigation Function

Artificial potential field-based methods that use attractive and repulsive potentials have been widely used to control multi-robot systems. Due to the existence of local minima when attractive and repulsive force are combined, robots can be trapped by local minima and are not guaranteed to reach the global minimum of the potential field. A navigation function is a particular category of potential functions where the potential field does not have local minima and the negative gradient vector field of the potential field guarantees almost global convergence to a desired destination, along with (guaranteed) collision avoidance, if the initial conditions do not lie within the sets of measure zero. Formally, a navigation function is defined as follows:

Definition 1 [13] [14] *Let \mathcal{F} be a compact connected analytic manifold with a boundary $\partial\mathcal{F}$, and q_d be a goal point in the interior of \mathcal{F} . A mapping $\varphi : \mathcal{F} \rightarrow [0, 1]$ is a Navigation Function, if it satisfies the following conditions: 1) smooth on \mathcal{F} (at least a C^2 function); 2) admissible on \mathcal{F} , (uniformly maximal on the manifold boundary $\partial\mathcal{F}$ and constraint boundary); 3) polar on \mathcal{F} , (q_d is a unique minimum); and 4) a Morse function, (critical points of the navigation function are non-degenerate).*

The second condition in Definition 1 establishes that the generated trajectories are collision-free, since the resulting vector field is transverse to the boundary of \mathcal{F} . The third point indicates that, using a polar function on a compact connected manifold with a boundary, all initial conditions are either brought to a saddle point or to the unique minimum q_d . The requirement that the navigation function is a Morse function ensures that the initial conditions that bring the system to saddle points are sets of measure zero [13]. Given this property, all initial conditions not within sets of measure zero are brought to the unique minimum.

The navigation function introduced in [13] and [14] ensures global convergence of the closed-loop system; how-

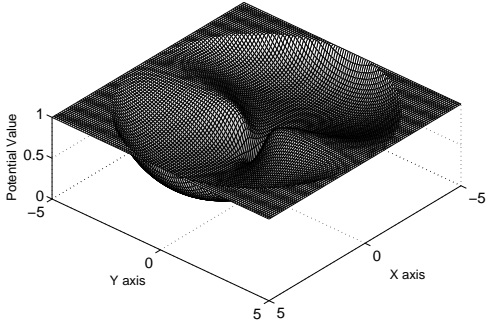


Figure 1. An example of a dipolar navigation function with a workspace of $R_w = 5$ and destination located at the origin with a desired orientation $\theta^* = 0$.

ever, the approach is not suitable for nonholonomic systems, since the feedback law generated from the gradient of the navigation function can lead to undesirable behaviors, which may be overcome by extending the original navigation function to a Dipolar Navigation Function in [23] and [24]. The flow lines created in the potential field resemble a dipole, so that the flow lines are all tangent to the desired orientation at the origin and utilized by the vehicle to achieve the desired orientation. An example of the dipolar navigation is shown in Fig. 3.1, where the potential field has a unique minimum at the destination (i.e., $p^* = [0, 0]^T$ and $\theta^* = 0$), and achieves the maxima at the workspace boundary of $R_w = 5$. Note that the surface $x = 0$ divides the workspace into two parts and forces all the flow lines to approach the destination parallel to the y -axis.

Inspired by the work in [23] and [24], the control strategy here is to develop a dipolar navigation function for the informed robot, which creates a feasible nonholonomic trajectory for the nonholonomic robot and guarantees the achievement of the specified destination with a desired orientation, while other follower robots aim to achieve consensus with the informed robot and maintain network connectivity by using only local interaction with neighboring robots. Following this idea, the dipolar navigation function is designed for the informed node $i \in \mathcal{V}_L$ as $\varphi_i^d(t) : \mathcal{F} \rightarrow [0, 1]$,

$$\varphi_i^d = \frac{\gamma_d}{(\gamma_d^\alpha + H_d \cdot \beta_d)^{1/\alpha}}, \quad (2)$$

where $\alpha \in \mathbb{R}^+$ is a tuning parameter. The goal function $\gamma_d(t) : \mathbb{R}^2 \rightarrow \mathbb{R}^+$ in (2) encodes the control objective of achieving the desired destination, which is specified by the distance from $p_i(t) \in \mathbb{R}^2$ to the destination $p^* \in \mathbb{R}^2$, and is designed as $\gamma_d = \|p_i(t) - p^*\|^2$. The

factor $H_d(t) \in \mathbb{R}^+$ in (2) creates a repulsive potential to align the trajectory of node i at the destination with the desired orientation. The repulsive potential factor is designed as

$$H_d = \varepsilon_{nh} + \left((p_i - p^*)^T \cdot n_d \right)^2, \quad (3)$$

where ε_{nh} is a small positive constant, and $n_d = \begin{bmatrix} \cos(\theta^*) \\ \sin(\theta^*) \end{bmatrix}^T \in \mathbb{R}^2$. A small disk area with radius $\delta_1 < R$ centered at node i is denoted as a collision region. To prevent a potential collision between node i and the workspace boundary, the function $\beta_d : \mathbb{R}^2 \rightarrow [0, 1]$ in (2) is designed as

$$\beta_d = \frac{1}{1 + e^{-\frac{2}{\delta_1} \log\left(\frac{1-\epsilon}{\epsilon}\right)(d_{i0} - \frac{1}{2}\delta_1)}} \quad (4)$$

where $0 < \epsilon \ll 1$ is a positive constant, and $d_{i0} \triangleq R_w - \|p_i\| \in \mathbb{R}$ is the relative distance of node i to the workspace boundary.

Since γ_d and β_d in (2) are guaranteed to not be zero simultaneously by Assumption 2, the navigation function candidate in (2) achieves its minimum of 0 when $\gamma_d = 0$ and its maximum of 1 when $\beta_d = 0$. Our previous work in [22] proves that the original navigation function with the form of $\varphi_i = \frac{\gamma_i}{(\gamma_i^\alpha + \beta_i)^{1/\alpha}}$ is a qualified navigation function. It is also shown in [12] that the navigation properties are not affected by the modification to a dipolar navigation with the design of (3), as long as the workspace is bounded, H_d in (2) can be bounded in the workspace, and ε_{nh} is a small positive constant. As a result, the decentralized navigation function φ_i^d proposed in (2) can be proven to be a qualified navigation function by following a similar procedure in [12] and [22]. From the properties of the navigation function, it is known that almost all initial positions (except for a set of measure zero points) asymptotically approach the desired destination.

To achieve consensus with the informed node while ensuring network connectivity and collision avoidance, a local interaction rule is designed for each follower node $i \in \mathcal{V}_F$ as $\varphi_i^f(t) : \mathcal{F} \rightarrow [0, 1]$,

$$\varphi_i^f = \frac{\gamma_i}{(\gamma_i^\alpha + \beta_i)^{1/\alpha}}, \quad (5)$$

where $\alpha \in \mathbb{R}^+$ is a tuning parameter. The goal function $\gamma_i(t) : \mathbb{R}^2 \rightarrow \mathbb{R}^+$ in (5) encodes the control objective of achieving consensus on the position between node i and neighboring nodes $j \in \mathcal{N}_i$, which is designed as

$$\gamma_i = \sum_{j \in \mathcal{N}_i} \|p_i(t) - p_j(t)\|^2. \quad (6)$$

Assume each node i has a collision region defined as a small disk with radius $\delta_1 < R$, and an escape region defined as the outer ring of the sensing area centered at the node with radius r , $R - \delta_2 < r < R$, where $\delta_2 \in \mathbb{R}^+$ is a predetermined buffer distance. Any node $j \in \mathcal{N}_i$ inside the collision region has the potential to collide with node i , and each edge formed by node i and $j \in \mathcal{N}_i$ in the escape region has the potential to break connectivity. To ensure collision avoidance and network connectivity, the constraint function $\beta_i : \mathbb{R}^{2N} \rightarrow [0, 1]$ in (5) is designed as

$$\beta_i = \prod_{j \in \mathcal{N}_i} b_{ij} B_{ij}, \quad (7)$$

by only accounting for nodes within its sensing area. Particularly, $b_{ij}(p_i, p_j) : \mathbb{R}^2 \rightarrow [0, 1]$ in (7) is a continuously differentiable sigmoid function, designed as

$$b_{ij} = \frac{1}{1 + e^{-\frac{2}{\delta_2} \log\left(\frac{1-\epsilon}{\epsilon}\right)(R - \frac{1}{2}\delta_2 - d_{ij})}}, \quad (8)$$

where $0 < \epsilon \ll 1$ is a positive constant. The designed b_{ij} ensures connectivity of nodes i and its neighboring nodes $j \in \mathcal{N}_i$ (i.e., nodes $j \in \mathcal{N}_i$ will never leave the sensing and communication zone of node i if node j is initially connected to node i).

Since collision avoidance among robots are only required in Ω_c , $B_{ij}(p_i, p_j) : \mathbb{R}^2 \rightarrow [0, 1]$ in (7) is designed as

$$B_{ij} = \frac{1}{1 + e^{-\frac{2}{\delta_1} \log\left(\frac{1-\epsilon}{\epsilon}\right)(d_{ij} - \frac{1}{2}\delta_1)}} \quad (9)$$

which indicates that collision avoidance is activated if the robots are in Ω_c , i.e., node i is repulsed from other nodes to prevent a collision in Ω_c . If the robots are in Ω_r , the collision avoidance is deactivated by removing B_{ij} from β_i in (7). Since Ω_r is defined by the distance to the destination and only the leader in the group is informed about the destination, the collision avoidance scheme designed in (9) is deactivated only when the leader is close enough to the destination in Ω_r .

That is β_i in (5) for $\forall i \in \mathcal{V}_F$ switches from $\beta_i = \prod_{j \in \mathcal{N}_i} b_{ij} B_{ij}$ to $\beta_i = \prod_{j \in \mathcal{N}_i} b_{ij}$ if the leader is close enough to the destination in Ω_r , so that collision avoidance among robots is not considered any more. The b_{ij} and B_{ij} are illustrated in Fig. 2. Note that the constraint function in (7) is designed to vanish whenever node i intersects with one of the constraints in the environment,

² The network will be proven to be connected all the time in the subsequent analysis, which implies that the distance between any two nodes is bounded by $R(N - 1)$. To ensure all followers are in Ω_r when the collision avoidance scheme is deactivated, the leader is required to deactivate the collision avoidance when its distance to the destination is less than $R_r - R(N - 1)$.

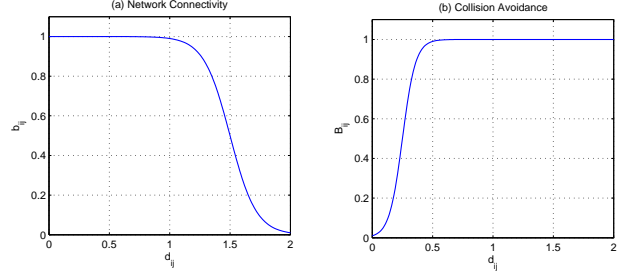


Figure 2. The plot of b_{ij} and B_{ij} with $\delta_1 = 0.5$, $\delta_2 = 1$, $R = 2$, and $\epsilon = 0.01$.

(i.e., if node i touches another node in Ω_c , or separates from adjacent nodes $j \in \mathcal{N}_i$ by distance of R_c). Since γ_i and β_i in (5) will not be zero simultaneously from their definitions, it is clear that φ_i^f achieves its minimum of 0 if $\gamma_i = 0$ (i.e., consensus is reached between node i and its immediate neighbors), and φ_i^f achieves its maximum of 1 if $\beta_i = 0$ (i.e., either the network connectivity or collision constraint is met).

3.2 Control Development

For brevity, φ_i is used to represent the potential function designed for each node i , where particularly $\varphi_i = \varphi_i^d$ in (2) if $i \in \mathcal{V}_L$, and $\varphi_i = \varphi_i^f$ in (5) if $i \in \mathcal{V}_F$. The desired orientation for any robot $i \in \mathcal{V}$, denoted by $\theta_{di}(t)$, is defined as a function of the negative gradient of the decentralized function φ_i as,

$$\theta_{di} \triangleq \arctan 2 \left(-\frac{\partial \varphi_i}{\partial y_i}, -\frac{\partial \varphi_i}{\partial x_i} \right), \quad (10)$$

where the mapping $\arctan 2(\cdot) : \mathbb{R}^2 \rightarrow \mathbb{R}$ denotes the four quadrant inverse tangent function, and $\theta_{di}(t)$ is confined to the region of $(-\pi, \pi]$. By defining $\theta_{di}|_{p^*} = \arctan 2(0, 0) = \theta_i|_{p^*}$, θ_{di} remains continuous along any approaching direction to the goal position. Based on the definition of θ_{di} in (10)

$$\nabla_i \varphi_i = -\|\nabla_i \varphi_i\| \begin{bmatrix} \cos(\theta_{di}) \\ \sin(\theta_{di}) \end{bmatrix}^T, \quad (11)$$

where $\nabla_i \varphi_i = \begin{bmatrix} \frac{\partial \varphi_i}{\partial x_i} & \frac{\partial \varphi_i}{\partial y_i} \end{bmatrix}^T$ denotes the partial derivative of φ_i with respect to p_i , and $\|\nabla_i \varphi_i\|$ denotes the Euclidean norm of $\nabla_i \varphi_i$. The difference between the current orientation and the desired orientation for robot i at each time instant is defined as

$$\tilde{\theta}_i(t) = \theta_i(t) - \theta_{di}(t), \quad (12)$$

where $\theta_{di}(t)$ is generated from the decentralized navigation function φ_i and (10). Based on the open-loop system in (1), the controller for each robot (i.e., the linear and angular velocity of robot i) is designed as

$$v_i = k_{v,i} \|\nabla_i \varphi_i\| \cos \tilde{\theta}_i, \quad (13)$$

$$\omega_i = -k_{w,i} \tilde{\theta}_i + \dot{\theta}_{di}, \quad (14)$$

where $k_{v,i}, k_{w,i} \in \mathbb{R}^+$ denote the control gains for robot i . The term $\dot{\theta}_{di}$ in (14) is determined as

$$\dot{\theta}_{di} = k_{v,i} \cos(\tilde{\theta}_i) \begin{bmatrix} \sin(\theta_{di}) \\ -\cos(\theta_{di}) \end{bmatrix}^T \nabla_i^2 \varphi_i \begin{bmatrix} \cos(\theta_i) \\ \sin(\theta_i) \end{bmatrix}, \quad (15)$$

where $\nabla_i^2 \varphi_i$ denotes the Hessian matrix of φ_i with respect to p_i . Note that the computation of $\nabla_i \varphi_i, \tilde{\theta}_i,$ and $\dot{\theta}_{di}$ only requires local position feedback and does not depend on communication with any neighbors, which highlights the decentralized nature of the controllers in (13) and (14). Although the switch of β_i will result in a discontinuity of the controller in (13) and (14) when the leader enters Ω_r from Ω_c , the controller remains continuous within Ω_r and Ω_c respectively. Substituting (13) into (1), the closed-loop system for robot i can be obtained as

$$\dot{p}_i = \begin{bmatrix} \dot{x}_i \\ \dot{y}_i \end{bmatrix} = k_{v,i} \|\nabla_i \varphi_i\| \cos \tilde{\theta}_i \begin{bmatrix} \cos \theta_i \\ \sin \theta_i \end{bmatrix}. \quad (16)$$

After using the fact that $\begin{bmatrix} \cos \theta_i & \sin \theta_i \end{bmatrix} \nabla_i \varphi_i = -\|\nabla_i \varphi_i\| \cos \tilde{\theta}_i$ from (11), the closed-loop error systems can be expressed as

$$\dot{p}_i = -k_{v,i} \nabla_i \varphi_i, \quad i \in \mathcal{V}. \quad (17)$$

4 Connectivity and Convergence Analysis

4.1 Connectivity Analysis

Theorem 1 *The controller in (13) and (14) ensures that the initially connected spanning tree structure is preserved when performing rendezvous for nodes with kinematics given by (1), as well as collision avoidance among robots in Ω_c .*

PROOF. The spanning tree structure in Assumption 1 ensures that there exists a path from the informed node to every follower node in $\mathcal{G}(0)$. To show every existing edge in the directed spanning tree in $\mathcal{G}(0)$ is preserved, consider a follower $i \in \mathcal{V}_F$ located at a position $p_0 \in$

\mathcal{F} that causes $\beta_i = 0$, which will be true when either only one node j is about to disconnect from node i or when multiple nodes are about to disconnect with node i simultaneously. If $\beta_i = 0$, the navigation function φ_i designed in (5) will achieve its maximum value. Driven by the negative gradient of φ_i in (17), no open set of initial conditions can be attracted to the maxima of the navigation function [14]. Therefore, every edge in \mathcal{G} is maintained and the directed spanning tree structure is preserved for all time.

Similar to the proof of the preservation of each link, if two nodes i and j are about to collide in Ω_c , that is $B_{ij}(p_i, p_j) = 0$ from (9), then the potential function φ_i in (5) will reach its maximum. Based on the properties of a navigation function driven by the vector field in (17), the system will not achieve its maximum. Hence, collision among nodes is avoided. \square

4.2 Convergence Analysis

Lemma 1 [25, 26] *Let \mathcal{G} be a directed graph of order n and $L \in \mathbb{R}^{n \times n}$ be the associated (non-symmetric) Laplacian matrix. Consider a linear system $\dot{x}(t) = -L(t)x(t)$, where $x(t) = [x_1, \dots, x_n]^T \in \mathbb{R}^n$. If the time-varying matrix $L(t) \in \mathbb{R}^{n \times n}$ is a piecewise continuous function of time with bounded elements, and \mathcal{G} has a directed spanning tree for all $t \geq 0$, then consensus is exponentially achieved, i.e., $x_1 = \dots = x_n$.*

Theorem 2 *Provided that \mathcal{G} has a spanning tree with the informed node as the root, the controller in (13) and (14) ensures that all robots with kinematics given by (1) converge to a common point with a desired orientation, in the sense that $\|p_i(t) - p^*\| \rightarrow 0$ and $|\tilde{\theta}_i(t)| \rightarrow 0$ as $t \rightarrow \infty \forall i \in \mathcal{V}$.*

PROOF. For the follower robots $i \in \mathcal{V}_F$, the term $\nabla_i \varphi_i$ in (17) is computed from (5) as

$$\nabla_i \varphi_i = \frac{\alpha \beta_i \nabla_i \gamma_i - \gamma_i \nabla_i \beta_i}{\alpha(\gamma_i^\alpha + \beta_i)^{\frac{1}{\alpha} + 1}}, \quad (18)$$

where $\nabla_i \gamma_i$ and $\nabla_i \beta_i$ are bounded in the workspace \mathcal{F} from (6) and (7), and $\nabla_i \gamma_i$ and $\nabla_i \beta_i$ in (18) can be determined as

$$\nabla_i \gamma_i = 2 \sum_{j \in \mathcal{N}_i} (p_i - p_j), \quad (19)$$

and

$$\nabla_i \beta_i = 2 \sum_{j \in \mathcal{N}_i} \left(\frac{\partial b_{ij}}{\partial d_{ij}} \right) \frac{\bar{b}_{ij}}{\|p_i - p_j\|} (p_i - p_j), \quad (20)$$

respectively, where $\bar{b}_{ij} \triangleq \prod_{l \in \mathcal{N}_i, l \neq j} b_{il}$. In (20), $\frac{\partial b_{ij}}{\partial d_{ij}}$ is

$$\frac{\partial b_{ij}}{\partial d_{ij}} = -\frac{\frac{2}{\delta_2} \log\left(\frac{1-\epsilon}{\epsilon}\right) e^{-\frac{2}{\delta_2} \log\left(\frac{1-\epsilon}{\epsilon}\right) (R - \frac{1}{2}\delta_2 - d_{ij})}}{\left(1 + e^{-\frac{2}{\delta_2} \log\left(\frac{1-\epsilon}{\epsilon}\right) (R - \frac{1}{2}\delta_2 - d_{ij})}\right)^2}, \quad (21)$$

which is negative, since δ_2 , $\frac{2}{\delta_2} \log\left(\frac{1-\epsilon}{\epsilon}\right)$, and $e^{-\frac{2}{\delta_2} \log\left(\frac{1-\epsilon}{\epsilon}\right) (R - \frac{1}{2}\delta_2 - d_{ij})}$ are all positive terms. Substituting (19) and (20) into (18), $\nabla_i \varphi_i$ is rewritten as

$$\nabla_i \varphi_i = \sum_{j \in \mathcal{N}_i} m_{ij} (p_i - p_j), \quad (22)$$

where

$$m_{ij} = \frac{2\alpha\beta_i - 2\left(\frac{\partial b_{ij}}{\partial d_{ij}}\right) \frac{\bar{b}_{ij}}{\|p_i - p_j\|} \gamma_i}{\alpha(\gamma_i^\alpha + \beta_i)^{\frac{1}{\alpha} + 1}} \quad (23)$$

is non-negative, based on the definitions of γ_i , β_i , α , \bar{b}_{ij} , and $\frac{\partial b_{ij}}{\partial d_{ij}}$ in (21). Using (17) and (22) yields the closed-loop system for each node i as:

$$\begin{cases} \dot{p}_i(t) = -k_{v,i} \nabla_i \varphi_i^d, & i \in \mathcal{V}_L \\ \dot{p}_i(t) = -\sum_{j \in \mathcal{N}_i} k_{v,i} m_{ij} (p_i - p_j), & i \in \mathcal{V}_F, \end{cases} \quad (24)$$

which can be rewritten in a compact form as

$$\dot{\mathbf{p}}(t) = -(\pi(t) \otimes I_2) \mathbf{p}(t) + \mathbf{F}_d, \quad (25)$$

where $\mathbf{p}(t) = [p_1^T, \dots, p_N^T]^T \in \mathbb{R}^{2N}$ denotes the stacked vector of p_i , $\mathbf{F}_d = [-k_{v,i} \nabla_i^T \varphi_i^d, 0, \dots, 0]^T \in \mathbb{R}^{2N}$ for $i = 1$ (recall that $\mathcal{V}_L = \{1\}$ from Section 2), I_2 is a 2×2 identity matrix, and the elements of $\pi(t) \in \mathbb{R}^{N \times N}$ are defined as

$$\pi_{ik}(t) = \begin{cases} \sum_{j \in \mathcal{N}_i} k_{v,i} m_{ij}, & i = k \\ -k_{v,i} m_{ik}, & k \in \mathcal{N}_i, i \neq k \\ 0, & k \notin \mathcal{N}_i, i \neq k. \end{cases} \quad (26)$$

Using the fact that m_{ij} is non-negative from (23), and $k_{v,i}$ is a positive constant gain in (13), the off-diagonal elements of $\pi(t)$ are negative or zero, and its row sums are zero. Hence, $\pi(t)$ is a Laplacian matrix. Since the informed node acts as the root in the spanning tree structure in \mathcal{G} , the first row of $\pi(t)$ is composed of all zeros, which indicates that the motion of the informed node is not dependent upon the motion of the followers. From Lemma 1 and the properties of the dipolar navigation function in (2), the first term in (25) indicates that $p_1 = \dots = p_N$, and the second term implies that $p_1 \rightarrow p^*$, and hence, $p_i \rightarrow p^* \forall i \in \mathcal{V}$.

Note that the properties of the developed dipolar navigation function in (2) ensure that the informed node

achieves the specified destination with the desired orientation. If the informed node always tracks its desired orientation θ_{di} and all the followers move along with the informed node, the group will achieve the destination with desired orientation. To show that $|\tilde{\theta}_i| \rightarrow 0$, we take the time derivative of $\tilde{\theta}_i(t)$ in (12) and use (1) to develop the open-loop orientation tracking error system as $\dot{\tilde{\theta}}_i = \omega_i - \dot{\theta}_{di}$. Using (14), the closed-loop orientation tracking error is

$$\dot{\tilde{\theta}}_i = -k_w \tilde{\theta}_i, \quad (27)$$

which has the exponentially decaying solution $\tilde{\theta}_i(t) = \tilde{\theta}_i(0) e^{-k_w t}$. \square

Remark 1 Since the network is proven to be connected in Theorem 1, the distance between any two nodes is bounded by $R(N-1)$, where R is the sensing radius and N is the number of nodes. By requiring the informed robot to move within a region with a distance to the workspace boundary greater than $R(N-1)$, the followers are guaranteed to avoid collision with the workspace boundary by achieving consensus with the informed robot.

Remark 2 The previous analysis is based on the simplification that only one informed node is considered. The result can be generalized to multiple informed nodes by using containment control theory. Containment control is a particular class of consensus problems in which all nodes are grouped into followers and leaders, and the followers, under the influence of leaders through local information exchange, converge to a desired region (i.e., a convex hull) formed by the leaders' states. Some recent results are reported in [27–29] for containment control. In our recent work in [30], a decentralized method is developed to influence followers in a social network to reach a common desired state (i.e., within a convex hull spanned by the leaders), while maintaining interaction among the followers and leaders. As a special case of [30], if each leader is assigned the same destination, the convex hull formed by leaders will shrink to the common destination, and the followers will converge to this desired destination. Therefore, following a similar approach in [30], all nodes can be proven to converge to the common destination, if multiple informed nodes are considered.

Remark 3 The switch of the controller (13) and (14) from Ω_c to Ω_r will not affect the stability of the system. Theorem 3.2 in [31] states that a switched nonlinear system is stable if the associated Lyapunov-like function V_i in each region Ω_i is nonincreasing, and V_i is also nonincreasing when switching occurs. It is proven that $\sum_i^N \varphi_i$ is a qualified Lyapunov function in [22], and following a similar approach as [22], $\sum_i^N \varphi_i$ is nonincreasing in Ω_c and Ω_r , respectively. To show that the Lyapunov function $\sum_i^N \varphi_i$ is nonincreasing when switching occurs, note that the denominator of φ_i^f in (5) is nondecreasing when

switching from Ω_c to Ω_r due to the fact that $B_{ij} \in [0, 1]$, which results in a nonincreasing φ_i^f . By invoking Theorem 3.2 in [31], the system remains stable when the switch occurs from Ω_c to Ω_r .

5 Simulation

The following numerical simulation demonstrates the performance of the controller developed in (13) and (14) in a scenario in which a group of six mobile robots with the kinematics in (1) are navigated to the common destination $p^* = [0 \ 0]^T$ with the desired orientation $\theta^* = 0$. The limited communication and sensing zone for each robot is assumed as $R = 2$ m and $\delta_1 = \delta_2 = 0.4$ m. The tuning parameter α in (2) is selected to be $\alpha = 1.2$. The workspace \mathcal{F} is a disk area centered at the origin with radius $R_w = 50$, and the rendezvous region is a disk area with radius $R_r = 11.5$. The collision avoidance scheme of the group is deactivated only when the informed robot is within a distance less than 1.5 to the common destination. The group of mobile robots is arbitrarily deployed in the workspace and forms a connected graph. The interaction between nodes is described by the network topology with a spanning tree as shown in Fig. 5, where the light dots denote the follower robots and the dark dot denotes the informed node. The informed node is randomly selected from the group, and is the only node aware of the desired destination p^* and orientation θ^* .

The control laws in (13) and (14) yield the simulation results shown in Fig. 5 and Fig. 5. Fig. 5 shows the trajectory for each robot, where the associated arrows indicate the initial or final orientation. To demonstrate the collision avoidance among robots and connectivity of existing links, the evolution of the inter-robot distance is plotted in Fig. 5. As shown in Fig. 5, the inter-robot distance decreases significantly for the first few seconds. Since the robots are moving in the collision free region initially, where collision avoidance is activated, the inter-robot distance stops to decrease when two robots are close to each other. Once the robots enter the rendezvous region, where collision avoidance is deactivated, the inter-robot distance decreases again to perform the desired rendezvous. Note that inter-robot distance is maintained less than the radius $R = 2$ m, which indicates that connectivity of the underlying graph is preserved.

6 Conclusion

A decentralized dipolar navigation function-based time-varying controller is developed to navigate a network of mobile robots to a common destination with a desired orientation while ensuring network connectivity and collision avoidance, using only local sensing information

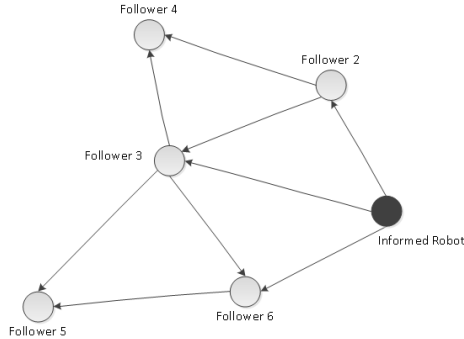


Figure 3. Network topology with directed edges indicating the directed interaction between two nodes.

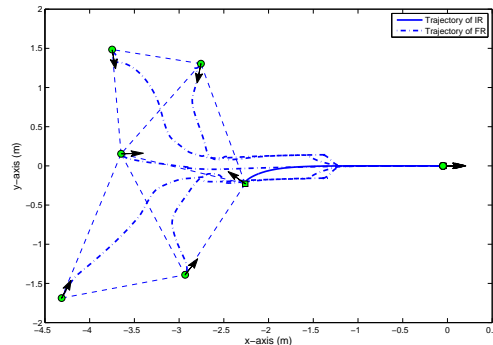


Figure 4. Plot of robot trajectories with solid line and dot-dash line indicating the trajectory of the informed robot (IR) and the follower robot (FR), respectively.

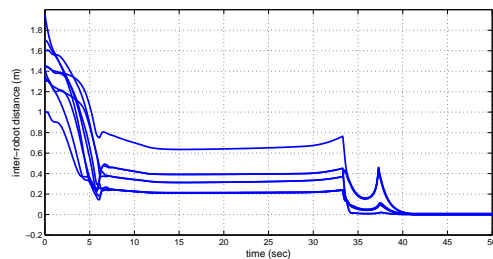


Figure 5. The evolution of inter-robot distance.

from one-hop neighbors. A distinguishing feature of the developed decentralized approach is that no inter-agent communication is required to complete the network consensus objective. Another distinguishing feature is that the more general problem of directed networks is considered, where only one robot is informed of the global objective while other robots coordinate their motions to perform the cooperative task by using local informa-

tion feedback from immediate neighbors. Although consensus among robots is ensured in this work, the rate of convergence is not considered. Generally, the rate of convergence depends on the network topology, which is a function of the roles of nodes (i.e., informed nodes or followers) and their interactions. A different set of informed nodes may lead to different convergence rates. Additional methods could be developed to optimize performance metrics such as the degree of connectivity and the convergence rate of the network in scenarios where the set of informed nodes can be determined and/or positioned a priori.

References

- [1] T. McLain and R. Beard, "Coordination variables, coordination functions, and cooperative-timing missions," *J. Guid. Contr. Dynam.*, vol. 28, no. 1, pp. 150–161, 2005.
- [2] E. Tekin and A. Yener, "The general Gaussian multiple-access and two-way wiretap channels: Achievable rates and cooperative jamming," *IEEE Trans. Inf. Theory*, vol. 54, no. 6, pp. 2735–2751, 2008.
- [3] Z. Lin, M. Broucke, and B. Francis, "Local control strategies for groups of mobile autonomous agents," *IEEE Trans. Autom. Control*, vol. 49, no. 4, pp. 622–629, 2004.
- [4] J. Lin, A. Morse, and B. Anderson, "The multi-agent rendezvous problem. Part 1: The synchronous case," *SIAM J. Control Optim.*, vol. 46, no. 6, pp. 2096–2119, 2007.
- [5] —, "The multi-agent rendezvous problem. part 2: The asynchronous case," *SIAM J. Control Optim.*, vol. 46, no. 6, pp. 2120–2147, 2007.
- [6] J. Cortés, S. Martínez, and F. Bullo, "Robust rendezvous for mobile autonomous agents via proximity graphs in arbitrary dimensions," *IEEE Trans. Autom. Control*, vol. 51, no. 8, pp. 1289–1298, 2006.
- [7] D. V. Dimarogonas and K. J. Kyriakopoulos, "On the rendezvous problem for multiple nonholonomic agents," *IEEE Trans. Automat. Control*, vol. 52, no. 5, pp. 916–922, May 2007.
- [8] H. Su, X. Wang, and G. Chen, "Rendezvous of multiple mobile agents with preserved network connectivity," *Syst. Control Lett.*, vol. 59, no. 5, pp. 313–322, 2010.
- [9] T. Gustavi, D. Dimarogonas, M. Egerstedt, and X. Hu, "Sufficient conditions for connectivity maintenance and rendezvous in leader–follower networks," *Automatica*, vol. 46, no. 1, pp. 133–139, 2010.
- [10] F. Xiao, L. Wang, and T. Chen, "Connectivity preservation for multi-agent rendezvous with link failure," *Automatica*, vol. 48, pp. 25–35, Jan. 2012.
- [11] Q. Hui, "Finite-time rendezvous algorithms for mobile autonomous agents," *IEEE Trans. Autom. Control*, vol. 56, no. 1, pp. 207–211, 2011.
- [12] S. Loizou and K. Kyriakopoulos, "Navigation of multiple kinematically constrained robots," *IEEE Trans. Robot.*, vol. 24, no. 1, pp. 221–231, 2008.
- [13] D. E. Koditschek and E. Rimon, "Robot navigation functions on manifolds with boundary," *Adv. Appl. Math.*, vol. 11, pp. 412–442, Dec 1990.
- [14] E. Rimon and D. Koditschek, "Exact robot navigation using artificial potential functions," *IEEE Trans. Robot. Autom.*, vol. 8, no. 5, pp. 501–518, Oct 1992.
- [15] G. Roussos, D. Dimarogonas, and K. Kyriakopoulos, "3D navigation and collision avoidance for a non-holonomic vehicle," in *Proc. Am. Control Conf.*, 2008, pp. 3512–3517.
- [16] T. Liu and Z. Jiang, "Distributed formation control of nonholonomic mobile robots without global position measurements," *Automatica*, vol. 49, no. 2, pp. 592–600, 2013.
- [17] W. Dong and J. Farrell, "Cooperative control of multiple nonholonomic mobile agents," *IEEE Trans. Autom. Contr.*, vol. 53, no. 6, pp. 1434–1448, 2008.
- [18] —, "Decentralized cooperative control of multiple nonholonomic dynamic systems with uncertainty," *Automatica*, vol. 45, no. 3, pp. 706–710, 2009.
- [19] L. Consolini, F. Morbidi, D. Prattichizzo, and M. Tosques, "Leader-follower formation control of nonholonomic mobile robots with input constraints," *Automatica*, vol. 44, no. 5, pp. 1343–1349, 2008.
- [20] Z. Kan, A. Dani, J. Shea, and W. E. Dixon, "Ensuring network connectivity for nonholonomic robots during rendezvous," in *Proc. IEEE Conf. Decis. Control*, Orlando, FL, 2011, pp. 2369–2374.
- [21] Z. Kan, J. Klotz, T.-H. Cheng, and W. E. Dixon, "Ensuring network connectivity for nonholonomic robots during decentralized rendezvous," in *Proc. Am. Control Conf.*, Montréal, Canada, June 2012, pp. 3718–3723.
- [22] Z. Kan, A. Dani, J. M. Shea, and W. E. Dixon, "Network connectivity preserving formation stabilization and obstacle avoidance via a decentralized controller," *IEEE Trans. Automat. Control*, vol. 57, no. 7, pp. 1827–1832, 2012.
- [23] H. Tanner and K. Kyriakopoulos, "Nonholonomic motion planning for mobile manipulators," in *IEEE International Conference on Robotics and Automation*, vol. 2, 2000, pp. 1233–1238 vol.2.
- [24] H. Tanner, S. Loizou, and K. Kyriakopoulos, "Nonholonomic navigation and control of cooperating mobile manipulators," *IEEE Trans. Robot. Autom.*, vol. 19, no. 1, pp. 53–64, Feb 2003.
- [25] L. Moreau, "Stability of continuous-time distributed consensus algorithms," in *Proc. IEEE Conf. Decis. Control*, 2004, pp. 3998–4003.
- [26] —, "Stability of multiagent systems with time-dependent communication links," *IEEE Trans. Autom. Control*, vol. 50, no. 2, pp. 169–182, February 2005.
- [27] G. Notarstefano, M. Egerstedt, and M. Haque, "Containment in leader-follower networks with switching communication topologies," *Automatica*, vol. 47, no. 5, pp. 1035–1040, 2011.
- [28] Y. Cao and W. Ren, "Containment control with multiple stationary or dynamic leaders under a directed interaction graph," in *Proc. IEEE Conf. Decis. Control*, 2009, pp. 3014–3019.
- [29] J. Mei, W. Ren, and G. Ma, "Distributed containment control for Lagrangian networks with parametric uncertainties under a directed graph," *Automatica*, vol. 48, no. 4, pp. 653–659, 2012.
- [30] Z. Kan, J. Klotz, E. Pasiliao, and W. E. Dixon, "Containment control for a social network with state-dependent connectivity," *Automatica*, 2012, submitted.
- [31] R. A. DeCarlo, M. S. Branicky, S. Pettersson, and B. Lennartson, "Perspectives and results on the stability and stabilizability of hybrid systems," *Proc. IEEE*, vol. 88, no. 7, pp. 1069–1082, 2000.